Appl. Sci. **2015**, *5*, 894-909; doi:10.3390/app5040894

OPEN ACCESS

applied sciences

ISSN 2076-3417

www.mdpi.com/journal/applsci

Article

Sidelobe Reduction in Non-Contiguous OFDM-Based Cognitive Radio Systems Using a Generalized Sidelobe Canceller

Atif Elahi [1,*], Ijaz Mansoor Qureshi [2,3,†], Zafar Ullah Khan [1,†] and Fawad Zaman [4,†]

[1] Department of Electronic Engineering, International Islamic University, Sector H-10, Islamabad 44000, Pakistan; E-Mail: zafarullah.phdee13@iiu.edu.pk

[2] Department of Electrical Engineering, Air University, Sector E-9, Islamabad 44000, Pakistan; E-Mail: imqureshi@mail.au.edu.pk

[3] Institute of Signal, Systems and Soft Computing (ISSS), Islamabad 44000, Pakistan

[4] Department of Electrical Engineering, COMSATS Institute of Information Technology, Attock Campus, Attock 43600, Pakistan; E-Mail: fawad@ciit-attock.edu.pk

† These authors contributed equally to this work.

* Author to whom correspondence should be addressed; E-Mail: atif.phdee40@iiu.edu.pk; Tel.: +92-332-9202431 or +92-310-9532282.

Academic Editor: Christos Verikoukis

Received: 19 August 2015 / Accepted: 9 October 2015 / Published: 21 October 2015

Abstract: In orthogonal frequency division multiplexing (OFDM), sidelobes of the modulated subcarriers cause high out-of-band (OOB) radiation, resulting in interference to licensed and un-licensed users in a cognitive radio system environment. In this work, we present a novel technique based on a generalized sidelobe canceller (GSC) for the reduction of sidelobes. The upper branch of the GSC consists of a weight vector designed by multiple constraints to preserve the desired portion of the input signal. The lower branch has a blocking matrix that blocks the desired portion and preserves the undesired portion (the sidelobes) of the input signal, followed by an adaptive weight vector. The adaptive weight vector adjusts the amplitudes of the undesired portion (the sidelobes) so that when the signal from the lower branch is subtracted from the signal from the upper branch, it results in cancellation of the sidelobes of the input signal. The effectiveness and strength of the proposed technique are verified through extensive simulations. The proposed technique produces competitive results in terms of sidelobe reduction as compared to existing techniques.

Keywords: cognitive radio; orthogonal frequency division multiplexing; generalized sidelobe canceller

1. Introduction

The rapid growth in wireless communication methods and devices is a major reason for spectrum scarcity. Cognitive radio (CR) is an encouraging solution to tackle such a problem and has received special attention in the research community. CR has the ability to dynamically permit secondary users (SU) to operate in those spectral domains that are not being used by the primary users (PU) at certain times and localities (interweave mode) [1–3]. Efficient techniques are needed at the transmitter side to control the shapes of the transmitted signal so that both SU and PU can share the same spectrum resources with minimum interference.

Orthogonal frequency division multiplexing (OFDM) is the best candidate for the CR [4–6], with the ability to divide the available wideband channel into multiple narrow band orthogonal channels/subcarriers and to transmit those subcarriers in parallel. Some attributes of OFDM include spectral efficiency, multipath delay spread, robustness to channel fading, *etc.* On the other hand, due to the large sidelobes of the OFDM subcarriers, CR based on OFDM experiences high out-of-band (OOB) radiation that may result in considerable interference with the adjacent bands used by either PU or SU. To tackle the OOB radiation problem, various techniques are proposed in the literature that can be categorized into two groups: time domain techniques and frequency domain techniques. Time domain techniques include filtering [7], which suffers from high complexity and lack of guard interval, and windowing [8,9], which expands the signal in time domain and results in intersymbol interference (ISI). Frequency domain techniques include adaptive symbol transition (AST) [10], which expands the signal by injecting additional samples within a specified power threshold between two transmission blocks to reduce the interference of these two blocks at definite frequencies, active interference cancellation (AIC) [11–13], where a few subcarriers lying at the border of the licensed user band are reserved for reducing the interference. These subcarriers, called cancellation subcarriers, are not used for data transmission, but to cancel the interference in a specific frequency range. In Cancellation carriers (CC) [14–16] method the authors propose the same technique as in AIC, but consider limiting the power to cancellation subcarriers. In both cases, finding the optimal complex values for cancellation carriers is a least squares (LS) optimization problem. In [17] the weights of cancellation carriers are calculated using Genetic Algorithm (GA) and Differential Evolution (DE). In [18] Selim, A., *et al.* propose a heuristic algorithm for calculating the weighting factors for the CC*s* with few computations. Active and null cancellation carriers (ANCC) [19] technique combine active and null cancellation carriers in the guard band. Subcarrier weighting (SW) [20] technique suppresses the sidelobes by weighting all the subcarriers with an optimal set of real-valued coefficients, advance subcarrier weightings (ASW) [21], in which Selim, A. and Doyle, L. propose a heuristic approach for sidelobe suppression for OFDM systems using subcarrier weighting, multiple choice sequence (MCS) [22], where the sequence of symbols carried by subcarriers is mapped to an optimal sequence that yields lower sidelobe interference, Constellation expansion (CE) [23–25] transmits symbols from a higher order constellation set and chooses the sequence that

results in the lowest possible sidelobe power level, Insertion of guard bands [26,27] where the interference is alleviated by adaptively deactivating the nearby subcarriers, providing flexible guard bands between licensed and un-licensed users and spectral precoding schemes [28–32] to reduce the interference by designing special precoder matrices, *etc.*

In this paper, we propose a novel technique for the reduction of OOB radiation in OFDM-based CR by using a generalized sidelobe canceller (GSC) at the transmitter of OFDM. It has been observed that so far in OFDM-based CR system, a GSC has not been used to tackle the OOB radiation problem. In the proposed technique, the signal is passed through two branches of a GSC. The upper branch consists of the weight vector designed by multiple constraints to preserve the desired portion of the signal, while the lower branch consists of a blocking matrix followed by a weight vector. The blocking matrix blocks the desired portion and preserves the undesired portions (sidelobes). The weight vector adjusts the undesired portion (sidelobes) in such a way that when subtracted from the signal of the upper branch, it results in significant cancellation of the sidelobes of the OFDM signal. We have compared the performance of the proposed technique with already existing techniques via simulations. The proposed technique achieves better suppression of the sidelobes as compared to the existing methods.

The remaining paper is arranged as follows: Section 2 contains the data model and Section 3 gives the proposed methodology. In Section 4, simulation results are carried out, while Section 5 concludes and gives future work recommendations.

2. Data Model

A general illustration of the non-contiguous orthogonal frequency division multiplexing (NCOFDM) transmitter that utilizes the proposed method is shown in Figure 1.

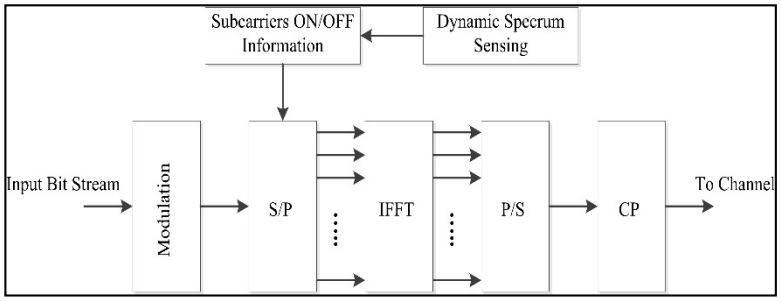

Figure 1. NCOFDM transmitter.

The input bit stream $x_n \in \mathbf{x} = [x_1, x_2, ..., x_N]^T$ is first modulated into symbols using Mary phase shift keying (PSK) or Mary quadrature amplitude modulation (QAM) $s_k \in \mathbf{s} = [s_1, s_2, ..., s_N]^T$. These modulated symbols are then divided into N parallel streams using serial to parallel (S/P) converter. An NCOFDM system has the ability to activate only those subcarriers that are located in vacant spectral bands detected by spectrum sensing techniques. These active subcarriers go through the inverse Fourier transform block following parallel to serial (P/S) converter. The cyclic prefix of length N_p is added to mitigate the impact of inter-symbol interference (ISI). The discrete time baseband transmitted NCOFDM signal that is to be transmitted in the time domain can be represented as [33–35]:

$$w_n = \frac{1}{N}\sum_{k=0}^{N-1} s_k e^{\frac{j2\pi kn}{N}}, \quad 0 \le n \le N-1 \tag{1}$$

The spectral shape of the individual subcarrier is obtained by Fourier transform of the time domain rectangular window, which is equal to the sinc function. The spectrum $u(f)$ of the k^{th} subcarrier is a sinc pulse modulated with data symbol s_k and is shifted to the respected subcarrier frequency f_k [6].

$$u_k(f) = s_k \sin c(\pi(f - f_k)T_o) \tag{2}$$

where f denotes the frequency, f_k is the center frequency of the k^{th} subcarrier, T_o is the NCOFDM symbol duration, and $(f - f_k)$ denotes the normalized center frequency of the k^{th} subcarrier. The spectrum of the transmitted NCOFDM signal is then the summation of the spectrum of all the active subcarriers, given by

$$U(f) = \sum_{k=0}^{N-1} u_k(f) \tag{3}$$

The signal given in Equation (3) has large sidelobes, which results in high OOB radiation, as shown in Figure 2 [14].

The main focus of this paper is to preserve the portion of NCOFDM signal from frequencies f_1 to f_N and to suppress the sidelobe, *i.e.*, the remaining portion of the NCOFDM signal.

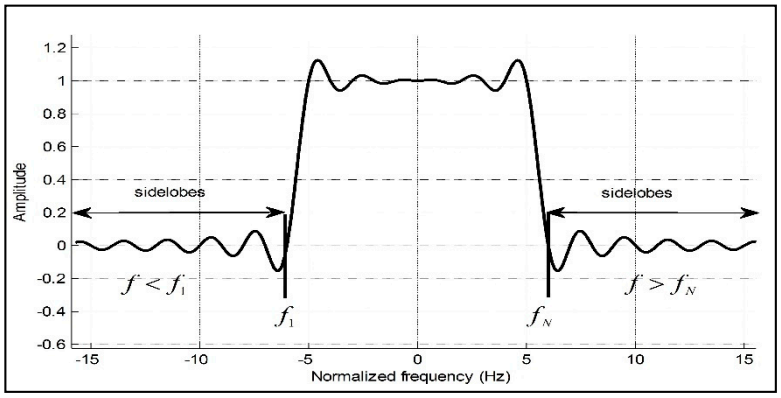

Figure 2. Transmitted NCOFDM signal in frequency domain.

3. Proposed Methodology

In this section, we propose a novel technique by using GSC at the transmitter of NCOFDM. GSC is the simplest version of linearly constrained minimum variance (LCMV), where the constrained optimization problem is converted into an unconstrained problem [36–38]. The block diagram of GSC is shown in Figure 3, having two branches, the upper branch and the lower branch. The upper branch is the main channel of the GSC, usually called a Fixed Beamformer (FBF). It consists of quiescent weight vector $\mathbf{w}_q$, which preserves the signal coming from SU, *i.e.*, the NCOFDM signal, and provides the necessary gain to the desired portion, *i.e.*, the region from f_1 to f_N satisfying the constraint, as shown in Figure 2. The lower branch consists of the blocking matrix **B** followed by an adaptive weight vector $\mathbf{w}_a$. The blocking matrix **B** blocks the desired portion of the signal and preserves the sidelobes of NCOFDM signal, as shown by region $f < f_1$ and $f > f_N$ in Figure 2. The adaptive weight vector $\mathbf{w}_a$ adjusts the amplitudes of the sidelobes. The sidelobes that are preserved and adjusted in the lower branch are then

subtracted from the signal of the upper branch, resulting in the signal of NCOFDM having suppressed or zero sidelobes.

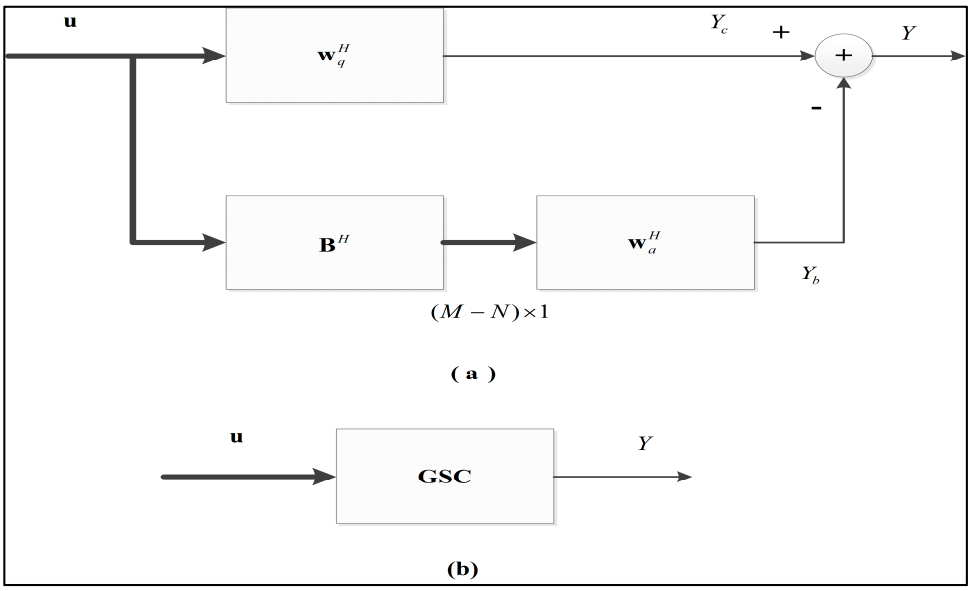

Figure 3. Generalized sidelobe canceller (GSC): (**a**) block diagram of GSC; (**b**) equivalent diagram of GSC.

To find the expressions for $\mathbf{w}_q$, $\mathbf{B}$ and $\mathbf{w}_a$, consider the NCOFDM signal given in Equation (3), represented by M samples, which are collected in the vector $\mathbf{u} = [\mathrm{u}_1, \mathrm{u}_2, \ldots \mathrm{u}_M]^T$ with uncorrelated elements. After passing through GSC it is given as

$$Y = \mathbf{w}^H \mathbf{u} \tag{4}$$

where the superscript H represents Hermitian and $\mathbf{w} = [\mathrm{w}_0, \mathrm{w}_1, \ldots, \mathrm{w}_{M-1}]^T$ is a weight vector with dimension $M \times 1$.

LCMV determines the optimal weight vector $\mathbf{w}^H$ that minimizes the output power having multiple linear constraints. The optimization problem for LCMV is given by:

$$\min_{\mathbf{w}} \mathbf{w}^H \mathbf{R}_\mathbf{u} \mathbf{w} \;\; s.t \;\; \mathbf{w}^H \mathbf{C} = \mathbf{g}^H \tag{5}$$

On solving Equation (5), we obtain:

$$\mathbf{w}_o^H = \mathbf{g}^H (\mathbf{C}^H \mathbf{R}_\mathbf{u}^{-1} \mathbf{C})^{-1} \mathbf{C}^H \mathbf{R}_\mathbf{u}^{-1} \tag{6}$$

where $\mathbf{R}_\mathbf{u} = E[\mathbf{u}\mathbf{u}^H] = \sigma^2 \mathbf{I}$ is the correlation matrix, with dimension $M \times M$, $\mathbf{I}$ is the identity matrix with dimension $M \times M$, σ^2 is the variance, while $\mathbf{C}$ is the constraint matrix with dimension $M \times N$, having N steering vectors given by Equation (7):

$$\mathbf{C} = [\mathbf{s}_1, \mathbf{s}_2, \ldots, \mathbf{s}_N] \tag{7}$$

where N represents the total number of frequencies in the desired portion of the signal, as shown in Figure 2; $\mathbf{s}_i = [s_1, s_2, \ldots s_M]^T$ is an i^{th} steering vector with dimension $M \times 1$ containing M samples of the i^{th} spectrum; and $\mathbf{g} = [1, 1, \ldots, 1]^T$ is called the gain vector with dimension $N \times 1$, which contains the desired gain related to each steering vector.

The effective implementation of LCMV is the division of a field with dimension $M \times M$ into the constraint subfield defined by columns of **C**, an $M \times N$ matrix, and an orthogonal subfield defined by columns of **B** an $M \times (M - N)$ matrix such that

$$\mathbf{C}^H\mathbf{B} = \mathbf{O} \tag{8}$$

where **O** is a null matrix with dimension $N \times (M - N)$ and **B** is a blocking matrix that blocks the desired portion of the NCOFDM signal.

Now consider the decomposition of $\mathbf{w}_o^H$ given in Equation (6) as

$$\mathbf{w}_o^H = \mathbf{w}_o^H\mathbf{P}_c - \mathbf{w}_o^H\mathbf{P}_o \tag{9}$$

where $\mathbf{w}_o^H\mathbf{P}_c$ represents the projection of $\mathbf{w}_o^H$ onto the constraint subfield and $\mathbf{w}_o^H\mathbf{P}_o$ represents the projection of $\mathbf{w}_o^H$ onto the orthogonal subfield. $\mathbf{P}_c$ and $\mathbf{P}_o$ are the projection matrices onto the constraint and orthogonal subfields with dimension $M \times M$ given by

$$\mathbf{P}_c = \mathbf{C}[\mathbf{C}^H\mathbf{C}]^{-1}\mathbf{C}^H \tag{10}$$

$$\mathbf{P}_o = \mathbf{B}[\mathbf{B}^H\mathbf{B}]^{-1}\mathbf{B}^H \tag{11}$$

where $\mathbf{P}_o$ can also be written as

$$\mathbf{P}_o = \mathbf{I} - \mathbf{P}_c \tag{12}$$

where **I** is an identity matrix with dimension $M \times M$.

The first component of Equation (9) represents the upper portion of GSC, which on solving becomes

$$\mathbf{w}_o^H\mathbf{P}_c = \mathbf{g}^H[\mathbf{C}^H\mathbf{R}_\mathbf{u}^{-1}\mathbf{C}]^{-1}\mathbf{C}^H\mathbf{R}_\mathbf{u}^{-1}\mathbf{C}[\mathbf{C}^H\mathbf{C}]^{-1}\mathbf{C}^H \tag{13}$$

$$\mathbf{w}_o^H\mathbf{P}_c = \mathbf{g}^H[\mathbf{C}^H\mathbf{C}]^{-1}\mathbf{C}^H \triangleq \mathbf{w}_q^H \tag{14}$$

where $\mathbf{w}_q^H$ is the quiescent weight vector having dimension $1 \times M$.

The second component of Equation (9) represents the lower portion of the GSC. On substituting the values for $\mathbf{w}_o^H$ and $\mathbf{P}_o$, Equation (9) becomes

$$\mathbf{w}_o^H\mathbf{P}_o = \mathbf{g}^H[\mathbf{C}^H\mathbf{R}_\mathbf{u}^{-1}\mathbf{C}]^{-1}\mathbf{C}^H\mathbf{R}_\mathbf{u}^{-1}\mathbf{B}[\mathbf{B}^H\mathbf{B}]^{-1}\mathbf{B}^H \tag{15}$$

As Equation (15) is not particularly useful for implementation, it is divided into two parts. The first part consists of blocking matrix **B**, and the second part consists of an adaptive weight vector $\mathbf{w}_a^H$ with dimension $1 \times (M - N)$.

The blocking matrix **B** can be constructed by first finding the $\mathbf{P}_o$ as given in Equation (12), then orthonormalizing $\mathbf{P}_o$ and choosing the first $(M - N)$ columns of the orthonormalized matrix that will be the resulting blocking matrix **B**, having the property given by

$$\mathbf{B}^H\mathbf{B} = \mathbf{I} \tag{16}$$

The output of the GSC as shown in Figure 3 after replacing $\mathbf{w}_o^H$ with $(\mathbf{w}_q - \mathbf{B}\mathbf{w}_a)^H$ will become:

$$Y = (\mathbf{w}_q - \mathbf{B}\mathbf{w}_a)^H\mathbf{u} \tag{17}$$

the output power of which is given by:

$$P = (\mathbf{w}_q - \mathbf{B}\mathbf{w}_a)^H \mathbf{R}_\mathbf{u} (\mathbf{w}_q - \mathbf{B}\mathbf{w}_a) \tag{18}$$

Solving Equation (18), we get the adaptive weight vector $\mathbf{w}_{a(opt)}$, given by the following equation:

$$\mathbf{w}_{a(opt)}^H = \mathbf{w}_q^H \mathbf{R}_\mathbf{u} \mathbf{B} (\mathbf{B}^H \mathbf{R}_\mathbf{u} \mathbf{B})^{-1} \tag{19}$$

4. Simulations and Results

In this section both the accuracy and the reliability of the proposed technique are discussed for the reduction of sidelobe suppression of the OFDM signal. The performance comparison of the proposed technique has been done in terms of normalized power spectral density (PSD) with already existing techniques in this area. Several cases have been discussed on the basis of spectral white spaces and its bandwidth between spectral white spaces. Throughout the simulations, the number of samples M is taken as 501, while the number of frequencies N in Case I is taken as 16, in Cases II and IV as 32, while in Case III and Case V, it is taken as 16, 32, 64, and 128, respectively.

4.1. Case I

In this case, we are considering a spectral white space that is not used by the PU and is available for the SU. The total number of OFDM subcarriers used by SU is 16 modulated with BPSK, whose power is normalized to $|d_n|^2 = 1$. The performance of the proposed technique is compared with different existing techniques, including CC [14], CC using GA and DE [17], ACC [18], and ASW [21]. In CC techniques, two CC*s* have been used either side of the data subcarriers, whereas in SW techniques all subcarriers are used for weighting. Figures 4 and 5 show the comparison of the proposed technique with the existing techniques in terms of PSD. It can be observed from Figures 4 and 5 that the existing techniques give a maximum of 36 dB improvement, while the proposed technique gives 92 dB improvement compared with the original OFDM spectrum. The proposed technique gives 58 dB improvement compared with the spectrum of OFDM using existing techniques.

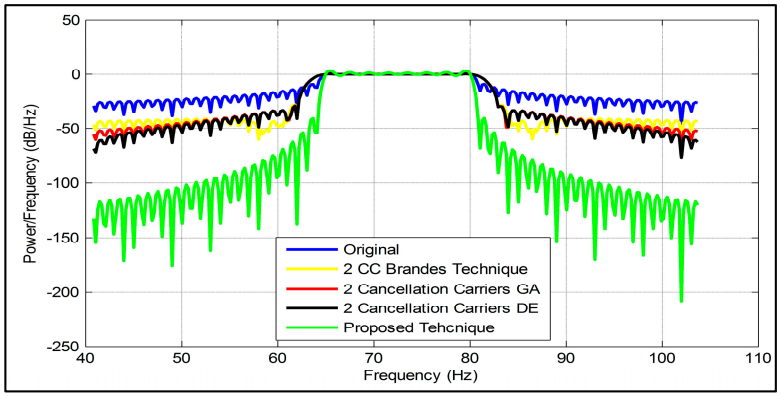

Figure 4. The PSD comparison between the proposed technique and existing techniques including SW, CC (Brandes), CC (GA), and CC (DE).

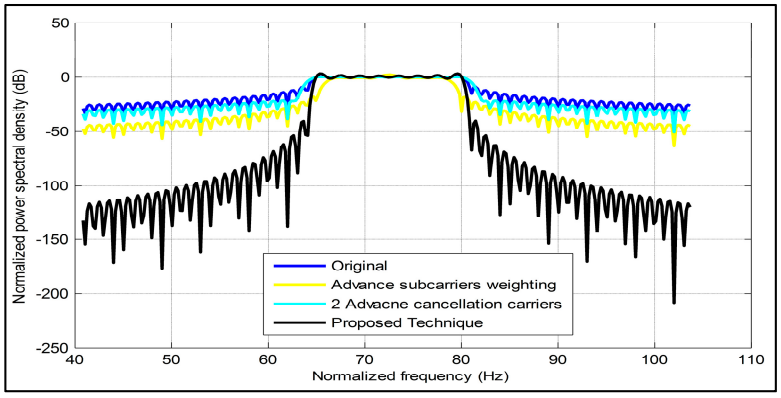

Figure 5. The PSD comparison between the proposed technique and existing techniques including ASW and ACC.

The comparison of the proposed technique with the existing ones is also given in Table 1, which shows the effectiveness of the proposed technique.

Table 1. Comparison of sidelobe suppression between existing and proposed techniques.

Techniques used	Sidelobe Powers	
	Left Side of the Data Subcarriers	**Right Side of the Data Subcarriers**
Original	−25 dB	−25 dB
CCs (Brandes)	−43 dB	−43 dB
CCs (GA)	−52 dB	−52 dB
CCs (DE)	−61 dB	−61 dB
ACCs	−30 dB	−30 dB
ASCW	−45 dB	−45 dB
Proposed technique	−117 dB	−117 dB

4.2. Case II

In this case, we are considering nine sub-bands mentioned as regions in Figures 6 and 7. We assume that regions I, III, V, VII, and IX are occupied by PU*s*, while regions II, IV, VI, and VIII are occupied by SU*s*. Each SU has an equal number of subcarriers, *i.e.*, 32 OFDM subcarriers modulated with BPSK, whose power is normalized to $|d_n|^2 = 1$. The bandwidth allocated to each PU is considered equal in all regions. The comparison of the proposed technique is done with already existing techniques including CC [14], CC using GA and DE [17], ACC [18], and ASW [21]. In CC techniques, two CC*s* have been used on either side of data subcarriers, while in the SW technique all subcarriers are taken into consideration. Figures 6 and 7 show the superiority of the proposed technique in terms of PSD, even in a spectrum-sharing scenario. The proposed technique performs well: it outclasses all these techniques and gets significant suppression in all regions.

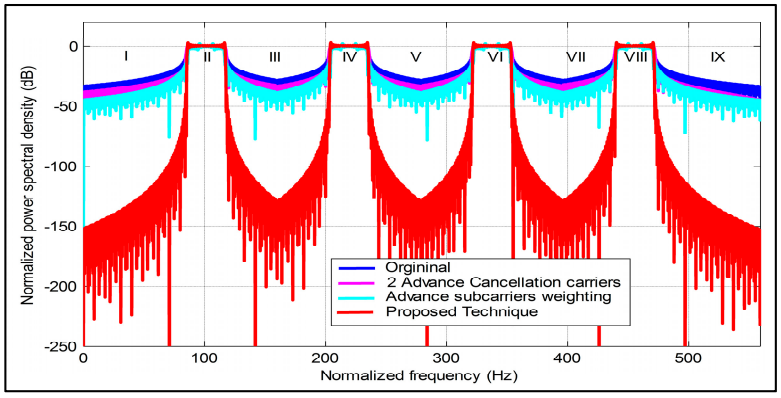

Figure 6. The PSD comparison between the proposed technique and existing techniques including ACC and ASW.

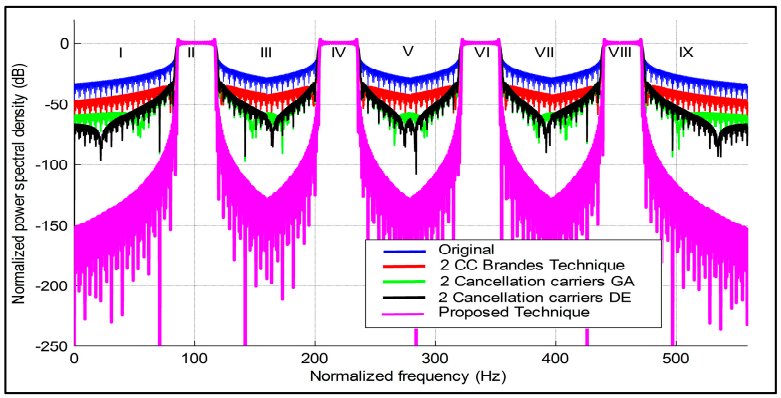

Figure 7. The PSD comparison between the proposed technique and existing techniques including CC (Brandes), CC (GA), and CC (DE).

The comparison of suppression of the sidelobe power level achieved in a spectrum-sharing scenario using the existing technique and our proposed technique are given in Table 2, which also shows the performance of our proposed technique in all regions of PU.

Table 2. Comparison of sidelobe suppression between existing and proposed techniques.

Techniques used	Sidelobe Power in Regions				
	I	**III**	**V**	**VII**	**IX**
Original	−33 dB	−28 dB	−28 dB	−28 dB	−33 dB
CCs (Brandes)	−47 dB	−42 dB	−42 dB	−42 dB	−47 dB
CCs (GA)	−59 dB	−57 dB	−57 dB	−57 dB	−59 dB
CCs (DE)	−80 dB	−70 dB	−70 dB	−70 dB	−80 dB
ACCs	−38 dB	−33 dB	−33 dB	−33 dB	−44 dB
ASCW	−45 dB	−38 dB	−38 dB	−38 dB	−45 dB
Proposed technique	−152 dB	−130 dB	−130 dB	−130 dB	−152 dB

4.3. Case III

In this case, we are considering the spectrum-sharing scenario consisting of a total of nine sub-bands mentioned as regions in Figures 8 and 9. We assume that regions I, III, V, VII, and IX are used by PU*s*,

while regions II, IV, VI, and VIII are used by SU*s*. An equal bandwidth is allocated to each PU, whereas it is unequal in the case of SU. The SU operating in region II has 16 subcarriers, region IV has 32, region VI has 64, and SU, operating in region VIII, has 128 subcarriers, modulated with BPSK, whose power is normalized to $|d_n|^2 = 1$. The performance of the proposed technique is compared with different existing techniques including CC [14], CC using GA and DE [17], ACC [18], and ASW [21].

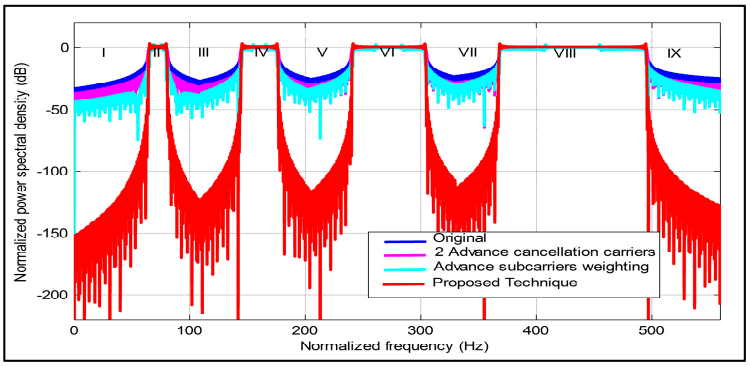

Figure 8. The PSD comparison between the proposed technique and existing techniques including ACC and ASW.

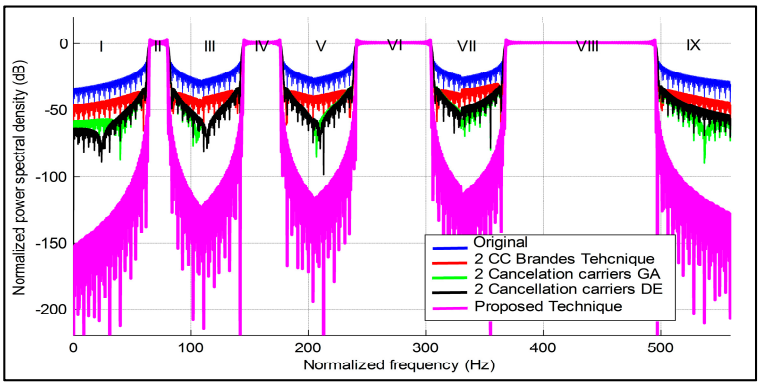

Figure 9. The PSD comparison between the proposed technique and existing techniques including CC (Brandes), CC (GA), and CC (DE).

In CC techniques, two CC*s* have been taken on either side of the data subcarriers, and in SW techniques all subcarriers are used for suppression. Figures 8 and 9 show that the proposed technique outclasses all these techniques and gives a significant suppression in all regions of the spectrum-sharing scenario.

Table 3. Comparison of sidelobe suppression between existing and proposed techniques.

Techniques used	Sidelobe Power in Regions				
	I	**III**	**V**	**VII**	**IX**
Original	−31 dB	−30 dB	−28 dB	−30 dB	−30 dB
CCs (Brandes)	−45 dB	−43 dB	−42 dB	−44 dB	−43 dB
CCs (GA)	−57 dB	−57 dB	−57 dB	−57 dB	−57 dB
CCs (DE)	−82 dB	−63 dB	−60 dB	−70 dB	−65 dB
ACCs	−36 dB	−34 dB	−34 dB	−35 dB	−34 dB
ASCW	−42 dB	−40 dB	−39 dB	−41 dB	−40 dB
Proposed technique	−142 dB	−135 dB	−130 dB	−140 dB	−136 dB

The performance comparison of reduction of OOB radiation in all PU regions between the existing and the proposed technique is given in Table 3. It clearly shows that the proposed technique gives significant reduction in sidelobes at all regions of PU and performs better than the rest.

4.4. Case IV

In this case, we are considering the spectrum-sharing scenario shown in Figures 10 and 11, consisting of nine sub-bands in total. Out of these nine, four are given to SU*s* designated by regions II, IV, VI, and VIII, while regions I, III, V, VII, and IX are given to PU*s*. Consider that the bandwidth allocated to all SU*s* is equal, while the bandwidths allocated to PU*s* are unequal. Each SU has 32 OFDM subcarriers. Figures 10 and 11 show the comparison of the proposed technique with already existing sidelobe suppression techniques including CC [14], CC using GA and DE [17], ACC [18], and ASW [21].

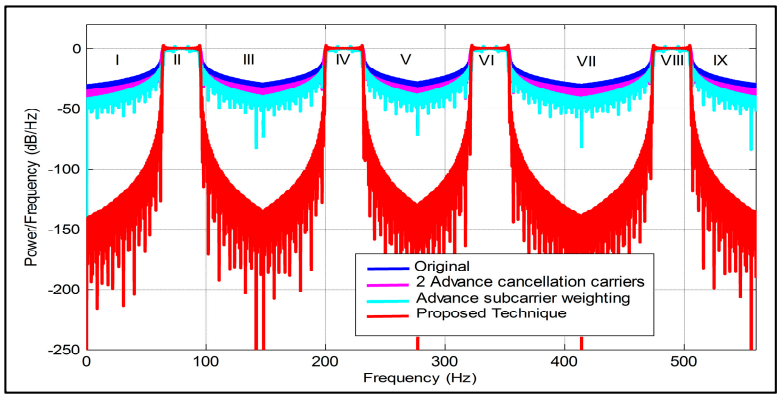

Figure 10. The PSD comparison between the proposed technique and existing techniques including ACC and ASW.

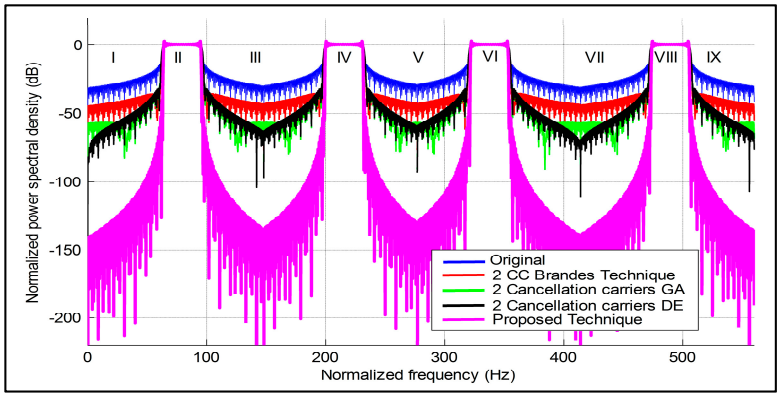

Figure 11. The PSD comparison between the proposed technique and existing techniques including CC (Brandes), CC (GA), and CC (DE).

In all CC techniques, two CC*s* have been taken on both sides of the data subcarriers. In terms of normalized PSD, Figures 10 and 11 show that clear reduction of OOB radiation is achieved in all regions of PU by the proposed technique.

Suppression of the sidelobe power level achieved at regions occupied by PU*s* using the existing and from the proposed technique is given in Table 4, which also shows the effectiveness the proposed technique.

Table 4. Comparison of sidelobe suppression between existing and proposed techniques.

Techniques used	Sidelobe Power in Regions				
	I	III	V	VII	IX
Original	−33 dB	−27 dB	−26 dB	−24 dB	−25 dB
CCs (Brandes)	−46 dB	−42 dB	−40 dB	−38 dB	−38 dB
CCs (GA)	−59 dB	−58 dB	−40 dB	−52 dB	−54 dB
CCs (DE)	−64 dB	−68 dB	−66 dB	−56 dB	−58 dB
ACCs	−37 dB	−32 dB	−30 dB	−28 dB	−30 dB
ASCW	−44 dB	−38 dB	−34 dB	−30 dB	−35 dB
Proposed technique	−152 dB	−125 dB	−118 dB	−114 dB	−127 dB

4.5. Case V

In this case, five out of nine sub-bands of unequal bandwidth are allocated to the PU*s*, designated as regions I, III, V, VII, and IX. Four sub-bands of unequal bandwidths allocated to SU*s*, designated as regions II, IV, VI, and VIII, are shown in Figures 12 and 13. We consider that the SU operating in regions II, IV, VI, and VIII has 16, 32, 64, and 128 OFDM subcarriers, respectively. The comparison of the proposed technique is done with the existing techniques. *i.e.*, CC [14], CC using GA and DE [17], ACC [18], and ASW [21]. Two CC*s* have been taken on both sides of the data subcarriers in all cancellation carrier techniques. In terms of normalized power spectral density, Figures 12 to 13 show that the proposed technique achieved significant suppression when compared to the existing techniques in all regions of PU*s*.

Suppression of sidelobe power level achieved in a spectrum-sharing scenario at regions allocated to PU*s*, using either the existing techniques or the proposed technique, is given in Table 5, which shows that the proposed technique gave outstanding results compared with the existing techniques in all regions of PU*s*.

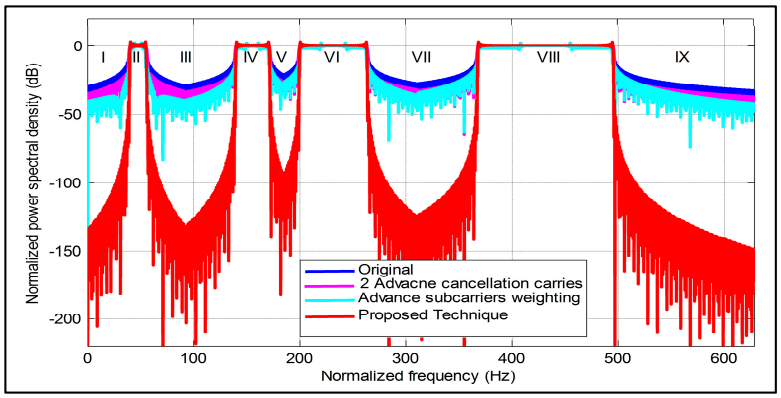

Figure 12. The PSD comparison between the proposed technique and existing techniques including ACC and ASW.

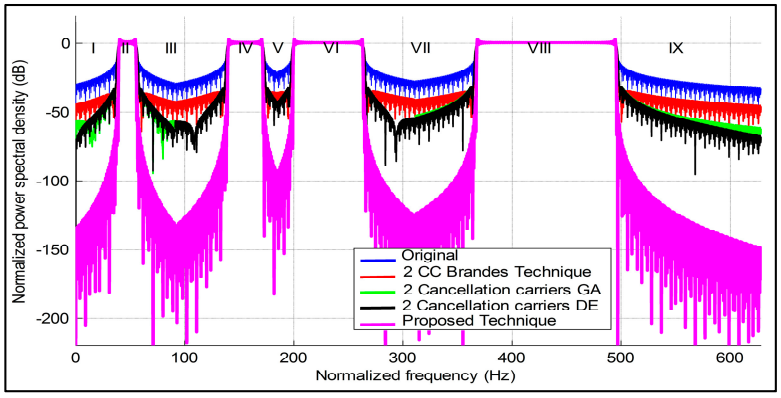

Figure 13. The PSD comparison between the proposed technique and existing techniques including CC (Brandes), CC (GA), and CC (DE).

Table 5. Comparison of sidelobe suppression between existing and proposed techniques.

Techniques used	Sidelobe Power in Regions				
	I	**III**	**V**	**VII**	**IX**
Original	−30 dB	−29 dB	−20 dB	−27 dB	−32 dB
CCs (Brandes)	−45 dB	−42 dB	−35 dB	−41 dB	−46 dB
CCs (GA)	−56 dB	−62 dB	−42 dB	−52 dB	−62 dB
CCs (DE)	−70 dB	−68 dB	−42 dB	−66 dB	−68 dB
ACCs	−35 dB	−34 dB	−26 dB	−32 dB	−38 dB
ASCW	−40 dB	−40 dB	−28 dB	−36 dB	−42 dB
Proposed technique	−135 dB	−133 dB	−95 dB	−125 dB	−150 dB

5. Conclusions and Future Work Recommendation

We have proposed a novel wave-shaping technique, GSC, for the reduction of sidelobes of OFDM signal. The proposed technique allows the desired portion of the signal to pass and blocks the undesired portion, *i.e.*, the sidelobes. The performance comparison of the proposed technique in different spectrum-sharing scenarios with already existing sidelobe suppression techniques is done through simulations, which show that the proposed technique achieves more than 90 dB reduction in sidelobes as compared to the existing techniques.

In the future, one can use the proposed approach for direction of arrival estimation of plane waves, as well as spherical waves. Moreover, the proposed scheme can also be tested for independent null steering.

Acknowledgements

The Authors thank Miss. Mehreen for her assistance and financial support of this research.

Author Contributions

Atif Elahi, Ijaz Mansoor Qureshi, Zafar Ullah Khan and Fawad Zaman contributed in the design of Generalized sidelobe canceller for the suppression of sidelobes in NCOFDM based cognitive radio systems, simulations of the results and preparation of manuscript.

Conflicts of Interest

The authors declare no conflict of interest.

References

1. Chen, K.C.; Peng, Y.J.; Prasad, N.; Liang, Y.C.; Sun, S. Cognitive radio network architecture: Part I–general structure. In Proceedings of the 2nd International Conference on Ubiquitous Information Management and Communication, Suwon, Korea, 31 January–1 February 2008; pp. 114–119.
2. Weiss, T.; Jondral, F.K. Spectrum pooling: An innovative strategy for the enhancement of spectrum efficiency. *IEEE Commun. Mag.* **2004**, *42*, S8–S14.
3. Meucci, F.; Cabral, O.; Velez, F.J.; Mihovska, A.; Prasad, N.R. Spectrum aggregation with multi-band user allocation over two frequency bands. In Proceedings of the Mobile WiMAX Symposium, 2009 (MWS'09), Napa Valley, CA, USA, 9–10 July 2009; pp. 81–86.
4. Mahmoud, H.; Yücek, T.; Arslan, H. OFDM for cognitive radio: Merits and challenges. *IEEE Wirel. Commun.* **2009**, *16*, 6–15.
5. Zhang, Y.; Leung, C. Resource allocation in an OFDM-based cognitive radio system. *IEEE Trans. Commun.* **2009**, *57*, 1928–1931.
6. Dikmese, S.; Loulou, A.; Srinivasan, S.; Renfors, M. Spectrum sensing and resource allocation models for enhanced OFDM based cognitive radio. In Proceedings of the 2014 9th International Conference on Cognitive Radio Oriented Wireless Networks and Communications (CROWNCOM), Oulu, Finland, 2–4 June 2014; pp. 360–365.
7. Noguet, D.; Gautier, M.; Berg, V. Advances in opportunistic radio technologies for TVWS. *EURASIP J. Wirel. Commun. Netw.* **2011**, *2011*, 1–12.
8. El-Saadany, M.S.; Shalash, A.F.; Abdallah, M. Revisiting active cancellation carriers for shaping the spectrum of OFDM-based cognitive radios. In Proceedings of the Sarnoff Symposium, 2009 (SARNOFF'09), Princeton, NJ, USA, 30 March–1 April 2009; pp. 1–5.
9. Sahin, A.; Arslan, H. Edge windowing for OFDM based systems. *IEEE Commun. Lett.* **2011**, *15*, 1208–1211.
10. Mahmoud, H.; Arslan, H. Sidelobe suppression in OFDM-based spectrum sharing systems using adaptive symbol transition. *IEEE Commun. Lett.* **2008**, *12*, 133–135.
11. Yamaguchi, H. Active interference cancellation technique for MB-OFDM cognitive radio. In Proceedings of the 34th European Microwave Conference, Amsterdam, The Netherlands, 12–14 October 2004; Volume 2, pp. 1105–1108.
12. Wang, Z.; Qu, D.; Jiang, T.; He, Y. Spectral sculpting for OFDM based opportunistic spectrum access by extended active interference cancellation. In Proceedings of the Global Telecommunications Conference, New Orleans, LA, USA, 30 November–4 December 2008; pp. 1–5.
13. Qu, D.; Wang, Z.; Jiang, T. Extended active interference cancellation for sidelobe suppression in cognitive radio OFDM systems with cyclic prefix. *IEEE Trans. Veh. Technol.* **2010**, *59*, 1689–1695.

14. Brandes, S.; Cosovic, I.; Schnell, M. Sidelobe suppression in OFDM systems by insertion of cancellation carriers. In Proceedings of the IEEE 62nd Vehicular Technology Conference, Dallas, TX, USA, 25–28 September 2005; Volume 1, pp. 152–156.
15. Pagadarai, S.; Wyglinski, A.M.; Rajbanshi, R. A sub-optimal sidelobe suppression technique for OFDM-based cognitive radios. In Proceedings of the Military Communications Conference, San Diego, CA, USA, 16–19 November 2008; pp. 1–6.
16. Kryszkiewicz, P.; Bogucka, H. Out-of-band power reduction in NC-OFDM with optimized cancellation carriers selection. *IEEE Commun. Lett.* **2013**, *17*, 1901–1904.
17. Elahi, A.; Qureshi, I.M.; Zaman, F.; Munir, F. Reduction of out of band radiation in non-contiguous OFDM based cognitive radio system using heuristic techniques. *J. Inf. Sci. Eng.*, in press.
18. Selim, A.; Macaluso, I.; Doyle, L. Efficient sidelobe suppression for OFDM systems using advanced cancellation carriers. In Proceedings of the 2013 IEEE International Conference on Communications (ICC), Budapest, Hungary, 9–13 June 2013; pp. 4687–4692.
19. Lopes, F.R.; Panaro, J.S. OFDM sidelobe suppression combining active and null cancellation carriers in the guard bands. In Proceedings of the 2013 SBMO/IEEE MTT-S International Microwave & Optoelectronics Conference (IMOC), Rio de Janeiro, Brazil, 4–7 August 2013; pp. 1–5.
20. Cosovic, I.; Brandes, S.; Schnell, M. Subcarrier weighting: A method for sidelobe suppression in OFDM systems. *IEEE Commun. Lett.* **2006**, *10*, 444–446.
21. Selim, A.; Doyle, L. Real-time sidelobe suppression for OFDM systems using advanced subcarrier weighting. In Proceedings of the 2013 IEEE Wireless Communications and Networking Conference (WCNC), Shanghai, China, 7–10 April 2013; pp. 4043–4047.
22. Cosovic, I.; Mazzoni, T. Suppression of sidelobes in OFDM systems by multiple-choice sequences. *Eur. Trans. Telecommun.* **2006**, *17*, 623–630.
23. Li, D.; Dai, X.; Zhang, H. Sidelobe suppression in NC-OFDM systems using constellation adjustment. *IEEE Commun. Lett.* **2009**, *13*, 327–329.
24. Pagadarai, S.; Rajbanshi, R.; Wyglinski, A.M.; Minden, G.J. Sidelobe suppression for OFDM-based cognitive radios using constellation expansion. In Proceedings of the Wireless Communications and Networking Conference, 2008 (WCNC 2008), Las Vegas, NV, USA, 31 March–3 April 2008; pp. 888–893.
25. Selim, A.; Ozgul, B.; Doyle, L. Efficient sidelobe suppression for OFDM systems with peak-to-average power ratio reduction. In Proceedings of the 2012 IEEE International Symposium on Dynamic Spectrum Access Networks (DYSPAN), Bellevue, WA, USA, 16–19 October 2012; pp. 510–516.
26. Weiss, T.; Hillenbrand, J.; Krohn, A.; Jondral, F.K. Mutual interference in OFDM-based spectrum pooling systems. In Proceedings of the 2004 IEEE 59th IEEE Vehicular Technology Conference, Milan, Italy, 17–19 May 2004; Volume 4, pp. 1873–1877.
27. Wireless LAN medium access control (MAC) and physical layer (PHY) specifications: High-speed physical layer in the 5GHz Band. Available online: http://simson.net/ref/1999/802.11b-1999.pdf (accessed on 19 October 2015).
28. Van de Beek, J. Orthogonal multiplexing in a subspace of frequency well-localized signals. *IEEE Commun. Lett.* **2010**, *14*, 882–884.

29. Ma, M.; Huang, X.; Jiao, B.; Guo, Y.J. Optimal orthogonal precoding for power leakage suppression in DFT-based systems. *IEEE Trans. Commun.* **2011**, *59*, 844–853.
30. Chung, C.D. Spectrally precoded OFDM. *IEEE Trans. Commun.* **2006**, *54*, 2173–2185.
31. Van de Beek, J.; Berggren, F. N-continuous OFDM. *IEEE Commun. Lett.* **2009**, *13*, 1–3.
32. You, Z.; Fang, J.; Lu, I.T. Combination of spectral and SVD precodings for out-of-band leakage suppression. In Proceedings of the 2013 IEEE Long Island Systems, Applications and Technology Conference (LISAT), Farmingdale, NY,USA, 3 May 2013; pp. 1–6.
33. Proakis, J.G.; Salehi, M. *Digital Communications*; McGraw-Hill: New York, NY, USA, 2008.
34. Goldsmith, A. *Wireless communications*; Cambridge University Press: New York, NY, USA, 2005.
35. Nee, R.V.; Prasad, R. *OFDM for Wireless Multimedia Communications*; Artech House: Norwood, MA, USA, 2000.
36. Haykin, S.S. *Adaptive Filter Theory*; Pearson Education India: Pataparganj, Delhi, India, 2008.
37. Van Trees, H.L. *Detection, Estimation, and Modulation Theory, Optimum Array Processing*; Wiley-Interscience: New York, NY, USA, 2004.
38. Khan, M.Z.U. New Methods for Null Steering in the Field of Adaptive Beamforming. Ph.D. Thesis, International Islamic University, Islamabad, Pakistan, 27 March 2014.